



Qualitative and quantitative determination of inclusions in high-carbon steel alloy (Class B) for rail wheel application by SEM/EDS analysis

by J.S. Moema*, S.M. Semenyat†, and C. Jones‡

Synopsis

It is well understood that to develop wagon wheels with higher abrasion resistance, fracture toughness, and fatigue resistance, steels with lower amounts of inclusions need to be used. Clean steels are produced with technologies that minimize the amount of inclusions in the microstructure. The demand for cleaner steels is high, and lowering of non-metallic oxide inclusions and controlling their morphology, composition, and size distribution is vital. Reduction of residual impurity elements such as sulphur, phosphorus, hydrogen, nitrogen, and trace elements is essential in the production of cleaner steel. Material cleanliness is vital for fatigue endurance, since oxide inclusions may act as stress concentrators and initiation points for fatigue cracks. To better understand the relationship between the cleanliness and toughness of the 34-inch cast wagon wheels, two samples of different levels of cleanliness were supplied for investigation. This paper presents the results of metallurgical analysis using scanning electron microscopy (SEM), energy-dispersive spectrometry (EDS), and mechanical tests for the pearlitic high-performance cast rail wagon wheel (identified as Class B) that are currently being used. The Charpy V-notch impact test results for the three samples from wagon wheels were compared. With the aid of SEM/EDS analysis system, non-metallic inclusions in these steels were detected, and it was possible to determine the position, size, shape, and composition of each particle. Alumina and manganese sulphide inclusions could be identified as the dominant inclusion types in the investigated samples. Fracture surface analysis of the Charpy specimen with high inclusions indicated that transgranular cleavage was the predominant fracture mode. Fractography of fracture surfaces of Charpy impact test samples also showed improvement of toughness properties on the clean sample.

Keywords

wagon wheels, steel cleanliness, inclusions, toughness, Charpy, SEM, EDS.

Introduction

A research team from a South African company that produces railway wagon wheels is involved in a research project to assess the cleanliness of 34-inch cast wagon wheels made from medium-high carbon steel grade and have a ferrite-pearlite microstructure summarized in ASTM A5041.

The producer desires to better understand the relationship between the cleanliness and impact toughness of the 34-inch Advanced

Casting Technique (ACT) wheels and to benchmark their Charpy impact fracture toughness according to ASTM standards. It is well understood that to develop wagon wheels with better abrasion resistance, fracture toughness, and fatigue resistance, cleaner steels need to be used. Clean steels are produced with technologies that minimize the amount of inclusions in the microstructure. These inclusions are classified into four types (A: sulphides, B: alumina (discontinuous string), C: silicate, and D: globular oxide). The inclusion content must conform to a quality that is not more severe than types $A \leq 2.5$; $B \leq 2.5$; $C \leq 2.5$, and $D \leq 2.5$ for the heavy series, and types $A \leq 2.5$; $B \leq 2.5$; $C \leq 2.5$; and $D \leq 2.5$ for the thin series¹.

The inclusion assessment must be performed in accordance with the requirements² of ASTM E45-87. This standard illustrates how to assess the inclusion level, and makes no pronouncements as to what level is appropriate for a particular application.

All over the world, the most prevalent wheel material grades fall under Class B or Class C according to the Association of American Railroads (AAR) specifications. A detailed comparison of mechanical properties and other characteristics between wrought and cast AAR Class C wheels with the same rim face hardness found no significant differences in strength, hardness distribution through cross-section, fatigue crack growth characteristics, and wear behaviour^{3,4}. It has been suggested that for these grades, keeping the carbon contents in the upper half of the specified range (0.57–0.67 per cent) and minor

* Mintek.

† University of Johannesburg.

‡ Scaw Metals of South Africa.

© The Southern African Institute of Mining and Metallurgy, 2013. ISSN 2225-6253. This paper was first presented at the, Ferrous and Base Metals Development Network Conference 2012, 15–17 October 2012, Mount Grace Country House and Spa, Magaliesburg, South Africa..

Qualitative and quantitative determination of inclusions in high-carbon steel alloy

additions of chromium and molybdenum (up to 0.20 per cent and 0.05 per cent, respectively) would be beneficial to achieve the minimum (specified) hardness of 321 BHN at the condemning diameter (on the rim)⁵, see Figure 1.

The performance of wagon wheels influences the safety and operating costs of railway transportation. Pressure is being applied on wheel manufacturers by the wagon wheel users to increase the life of wheels^{6,7}. Wagon wheels have a limited life because they suffer from rolling contact fatigue (RCF) and shelling. Failure can be caused by poor production methods. Cleaner steels can be produced using advanced technologies, but these are expensive. Testing of the cleanliness of wagon wheels according to the Association of American Railroads (AAR) specifications is performed overseas. This takes time and is a costly exercise for the rail industry. The development of a method that can show the influence of inclusions on the mechanical and wear properties of the wagon wheel would prove to be very useful for the South African railway industry⁸. Research has shown that the presence of non-metallic inclusions (particularly the hard ones such as alumina (Al_2O_3) and complex oxides) and voids has detrimental effects on mechanical properties of steels^{9,10}.

In this paper, a high-carbon steel alloy (Class B) used in the manufacture of wagon wheels was investigated. Two wagon wheels with differing levels of cleanliness were produced from the Class B steel alloy. Samples from these alloys were analysed metallographically using optical microscopy and scanning electron microscopy (SEM), which clearly revealed the three-dimensional morphology and the composition of each inclusion examined.

Experimental technique

Two samples from railway wheels were supplied by a local wagon wheel producer for metallurgical investigation. These two samples belonged to wagon wheels that were manufactured from different heats. One sample was removed from a good batch and the other from a wheel that was rejected during the quality control test, which showed a large surface inclusion (Figure 2). The investigation was limited to chemical analysis, microstructural analysis, Charpy impact tests, and fractography by SEM.

Cross-sections were removed from the supplied samples (i.e. good and rejected) using an abrasive cut-off machine. The specimens were then taken for chemical analysis using spark emission spectrometry, and the chemical composition was compared to that of a reference Class B alloy. Two specimens were removed from the rim of the two sectioned wheels supplied. The sectioned specimens were prepared for metallographic examination. The specimens were mechanically polished to a $1\mu m$ finish using a diamond paste. The sections were studied in the as-polished condition for inclusion content using a Nikon optical microscope. Thereafter, the sections were micro-etched with 2 per cent Nital in order to reveal the microstructures.

To supplement optical metallography, the specimens were also examined using a scanning electron microscope equipped with energy-dispersive spectrometry (EDS) capability. Some of the samples examined by SEM were deeply etched to better reveal the pearlite morphology. EDS was used to determine the compositional variations within the microstructure (i.e. identification of inclusion types).

Three Charpy impact specimens were removed from the two sectioned wagon wheels in both the circumferential and the axial directions and tested using a Tinius Olsen impact tester according to ASTM E23-72¹¹. The principal measurement from the impact test is the energy absorbed in fracturing the specimen. The fracture surfaces of the wheel specimens after the impact test were examined by SEM-EDS to reveal the fracture mechanism and analyse the inclusions.

Results and discussion

Chemical analysis

The chemical composition of the investigated alloy and the specification¹ as per ASTM A504 is shown in Table 1. It is apparent from the comparison that the wheels have similar composition to class B wheels (ASTM-A504). The carbon (C) and manganese (Mn) contents of the rejected sample are slightly higher than that of the good one.

Microstructural analysis

The samples were also studied in the as-polished condition to investigate the cleanliness (i.e. amount of inclusions

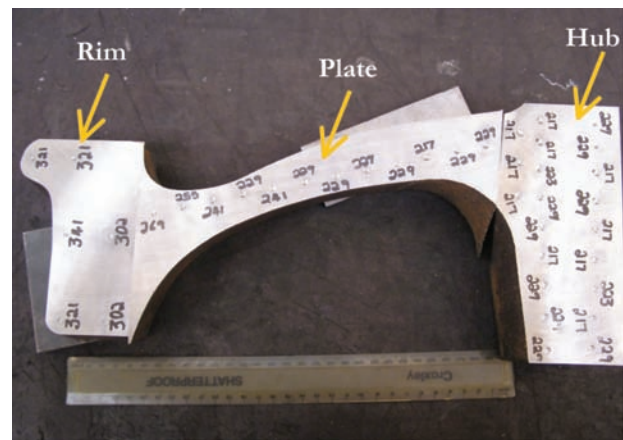


Figure 1—Photograph showing a section of a railroad freight wagon wheel (rim, plate, and hub)

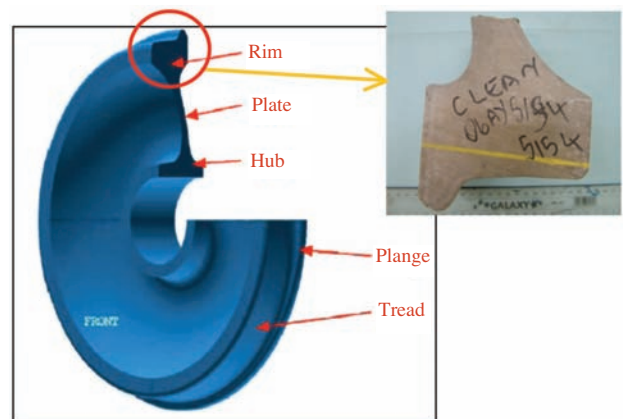


Figure 2—Photograph showing a section of the wagon wheel (rim) removed from good batch

Qualitative and quantitative determination of inclusions in high-carbon steel alloy

Table 1
The chemical composition of the supplied samples, wt. %

Alloy	Element, wt%								
	C	Si	Mn	P	S	Cr	Ni	Cu	Mo
Class B specification	0.57–0.67	0.15 min	0.6–0.90	0.05 max	0.05 max	0.25 max	0.25 max	0.35 max	0.10 max
Good/clean sample	0.58	0.71	0.69	0.002	0.020	0.16	0.06	0.16	0.01
Rejected sample	0.66	0.65	0.79	0.009	0.014	0.16	0.07	0.10	0.01

present). Figures 3 and 4 show the as-polished micrographs of the clean and rejected samples respectively. The clean sample has fewer inclusions which are homogeneously distributed throughout the cross-section as compared to the rejected sample. The oxide inclusions are globular in shape; this morphology is preferable since their effect on mechanical properties is moderate. Figure 3 shows the micrograph of the rejected sample, which reveals inclusions such as oxides (black dots) and some sulphides (grey). It contains a high amount of inclusions compared to the clean sample.

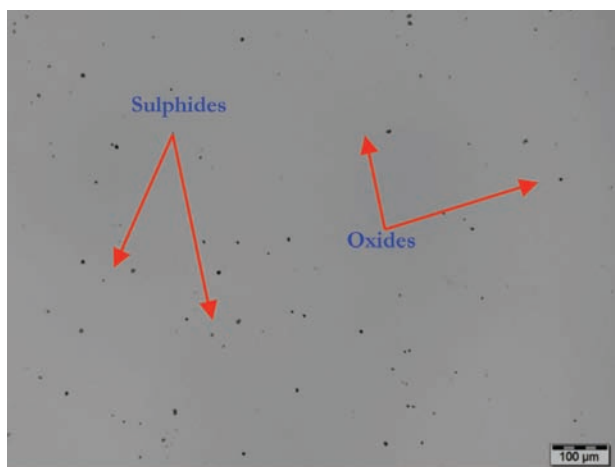


Figure 3—Micrograph of a clean sample showing lower amount of inclusions such as oxides (black dots) and sulphides (grey)

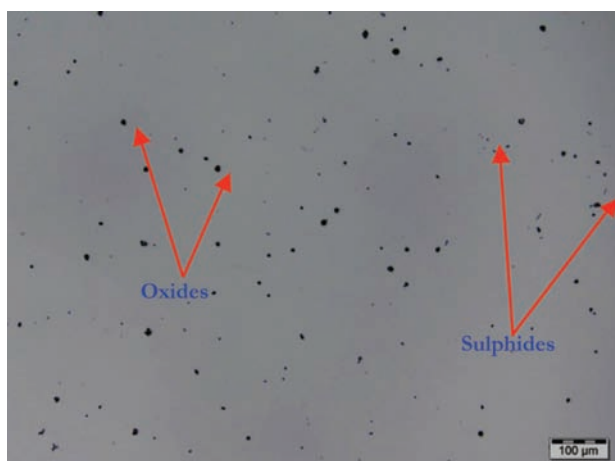


Figure 4—Micrograph of a rejected sample showing high amount of inclusions such as oxides (black dots) and sulphides (grey)

The samples were also studied in the etched condition to investigate the microstructure. The target microstructure of the heat-treated rail wheel alloy, according to specification, must consist of 95 per cent pearlite and 5 per cent ferrite. The microstructure with this phase mix is expected to yield the required mechanical properties. The microstructures of the supplied clean and rejected samples (removed near the rim) at low and high magnification are shown in Figures 5 to 8. The microstructure consists of fine grains of pearlite and

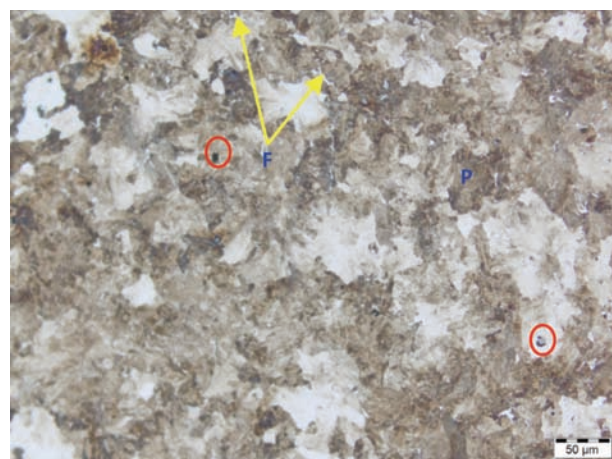


Figure 5—The microstructure of a clean sample (Class B alloy) on the rim showing fine grains of pearlite (P), ferrite (F – white phase), and low amount of inclusion (black spots)



Figure 6—The microstructure of a clean sample (Class B alloy) on the rim at a higher magnification than Figure 4, showing pearlite (P) and ferrite (F – white phase)

Qualitative and quantitative determination of inclusions in high-carbon steel alloy



Figure 7—The microstructure of a rejected sample (Class B alloy) on the rim showing fine grains of pearlite (P) and ferrite (F – white phase)



Figure 8—The microstructure of a rejected sample (Class B alloy) on the rim at a higher magnification than Figure 7 showing pearlite (P), ferrite (F – white phase), and inclusions (black spots indicated by the arrows)

ferrite (white phase). Pearlite is a mixture of ferrite and cementite in which the two phases are formed from austenite in an alternating lamellar pattern. Formation of pearlite occurs during relatively slow cooling from the austenite region and depends on the steel composition.

Figures 5 and 7 shows the presence of pearlite with traces of hypo-eutectoid ferrite along the grain boundaries. The reason for this combination of phases in the microstructure is to have the advantage of the well-known high wear resistance of pearlite and to prevent the formation of pro-eutectoid cementite along the grain boundaries. This may increase fracture toughness and reduce cracking propensity along the grain boundaries, and (ideally) shelling.

Scanning electron microscopy (SEM)

With the help of the high-resolution SEM/EDS analysis system, non-metallic micro-inclusions in the supplied steel samples were detected on a metallographically prepared surface area. It was possible to determine the position, size,

shape, and composition of each inclusion particle. Manganese, alumina, common spinel, sulphide, and oxisulphide inclusions could be identified as the dominant inclusion types in the supplied steel. Figures 9 to 12 depict the SEM microstructures and EDS spectra of the clean and dirty/rejected samples, showing the shape, size, and type of inclusions.

The EDS spectrum of the clean sample shows sulphur and manganese and traces of calcium, possibly from deoxidizer during steelmaking. The EDS spectrum of the rejected sample shows major sulphur, manganese, and oxygen contents and traces of aluminium and silicon, again possibly from the deoxidizer during steelmaking. Some inclusions are observed on the polished surfaces of the specimens, and EDS analysis has shown that these inclusions are some kind of sulphur compound. The defects or inclusions analysed are manganese sulphides. Aluminium is required for killing the molten steel, but excess quantities of aluminium produce alumina inclusions which are very hard and deleterious to the steel's mechanical properties.

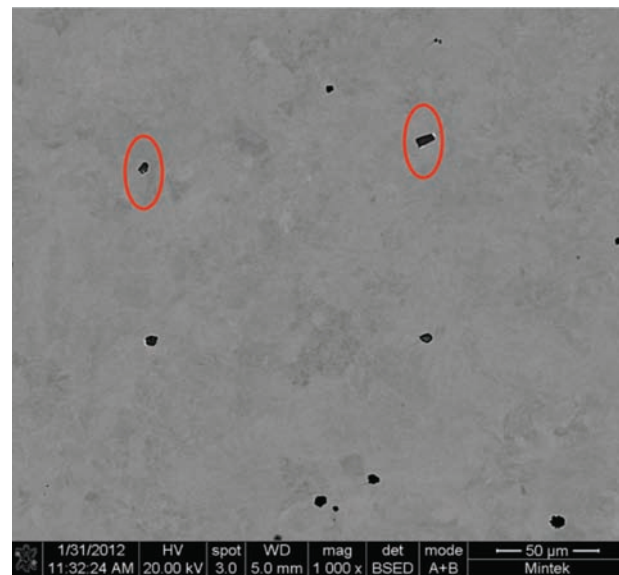


Figure 9—SEM micrograph of a clean sample on the rim showing distribution of inclusions (dark particles)

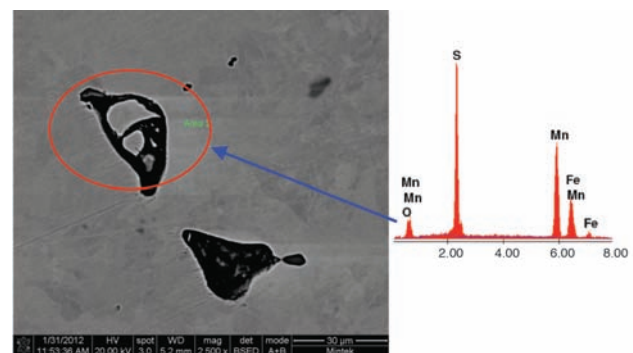


Figure 10—SEM micrograph of a clean sample from the rim at a higher magnification than Figure 9, showing the shape, size, and type of inclusions (dark phase)

Qualitative and quantitative determination of inclusions in high-carbon steel alloy

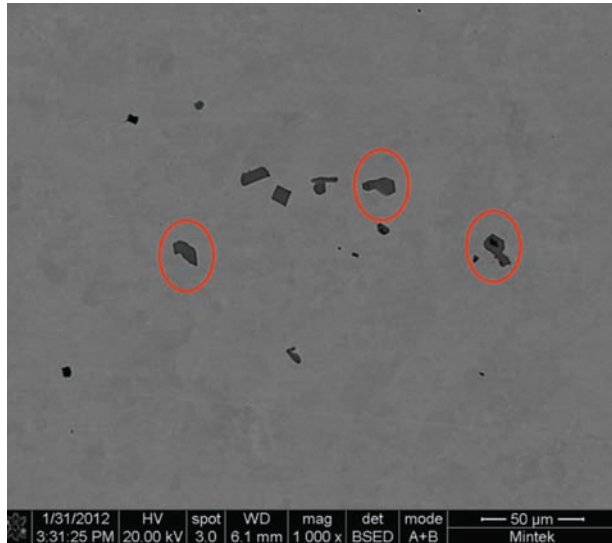


Figure 11—SEM micrograph of a rejected sample on the rim showing distribution of inclusions (dark phase)

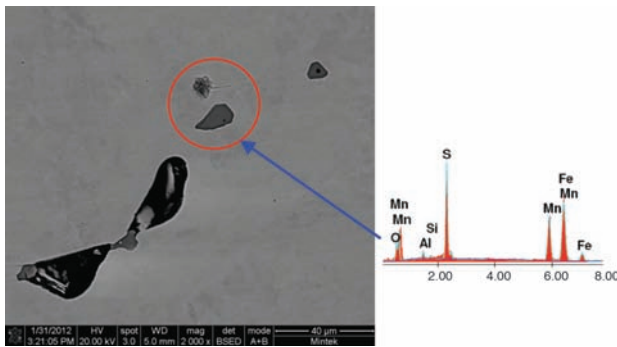


Figure 12—SEM micrograph of a rejected sample on the rim at a high magnification than Figure 11, showing the shape, size, and type of inclusions (dark phase)

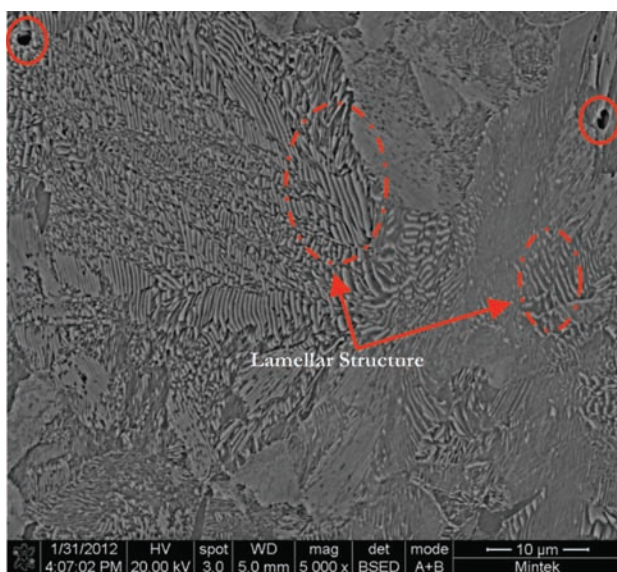


Figure 13—SEM micrograph of a clean sample machined from the wheel rim showing the pearlite structure (lamellar structure comprising ferrite and cementite) and inclusions

The microstructure of the etched clean sample was studied using SEM. Figures 13 and 14 show the lamellar morphology of the pearlite. As well as the significant higher pearlite content of the wheel steel, the ferrite areas and cementite lamellae spacing could be clearly identified.

Impact testing

The impact toughness test results of the clean and rejected samples tested at room temperature are shown in Table II. According to the specification, the Charpy V notch (CVN) impact test, particularly for the cast wheels, is performed for information only. The clean sample shows higher impact values compared to the rejected samples. The amount and type of inclusions present in the rejected sample led to the reduction in the Charpy impact toughness. The specimen extracted from an axial direction of the samples showed a lower impact toughness values compared to circumferential specimen, and are below the specification for Class B wheels¹².

Fractography

The fracture surfaces of the clean sample after impact testing are characterized essentially by typical transgranular cleavage, without any evidence of the presence of striation marks (compare microfractographic results in Figures 15 to 17). An additional microfractographic feature is the presence of a stepped fracture topography, due to the delamination of the lamellar microstructure (ferrite/cementite interface). This indicates that the material is brittle. These observations clearly indicate that the resulting fracture topography of a pearlitic microstructure depends on the relationship between the orientation of the pearlitic colony and the load direction. As consequence, adjacent pearlitic colonies may display distinct fractographic features.

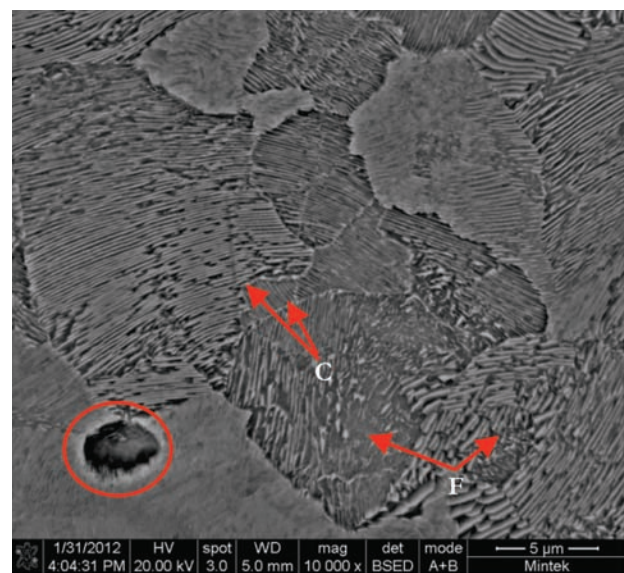


Figure 14 – SEM micrograph of a clean sample machined from the wheel rim showing the pearlite structure (lamellar structure comprising ferrite (F) and cementite (C)), and an inclusion

Qualitative and quantitative determination of inclusions in high-carbon steel alloy

Table II

Charpy V notch impact test results of the samples in circumferential and axial direction

Alloy	Specimen 1 (J)	Specimen 2 (J)	Specimen 3 (J)	Average (J)
Class B wheels (ASTM A504)	-	-	-	20
Clean (circumferential)	12	14	12	12.7
Clean (axial)	12	11	12	11.7
Rejected (circumferential)	10	10	11	10.3
Rejected (axial)	12	8	7	9

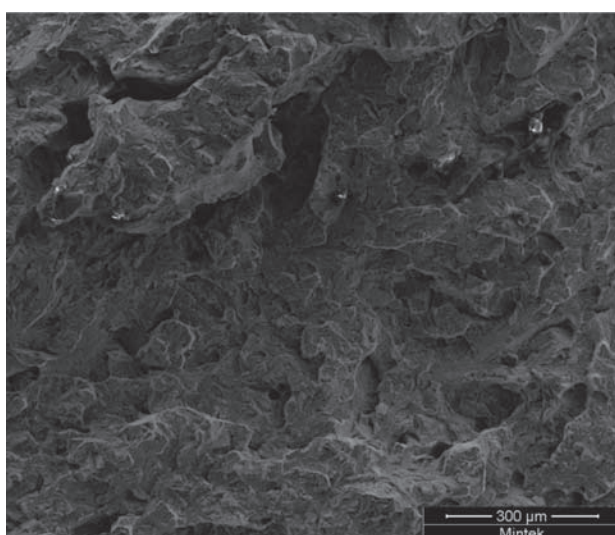


Figure 15—SEM fracture topography of a clean sample showing the fracture surface that consists essentially of transgranular cleavage fracture

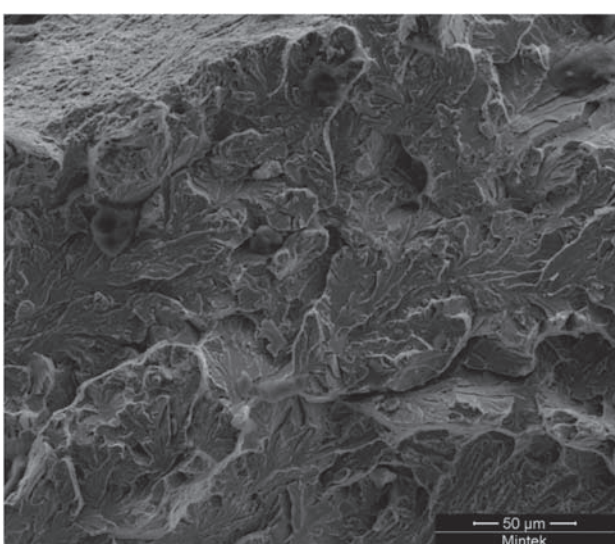


Figure 16—SEM fracture topography of a clean sample at a higher magnification than Figure 14, showing transgranular cleavage fracture

Conclusions

- The chemical composition of the alloy tested conforms to the requirements specification

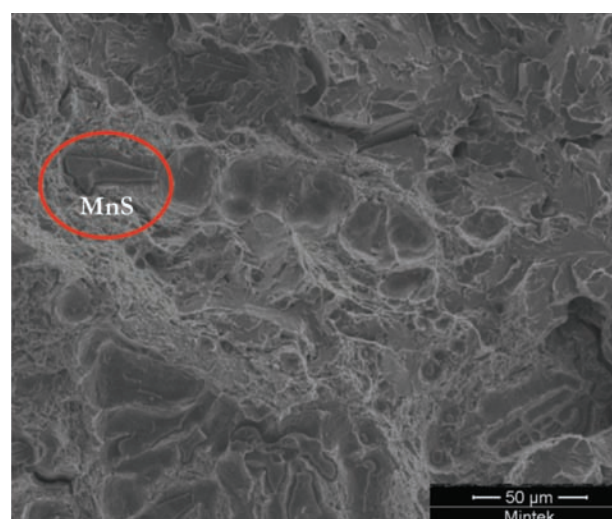


Figure 17—SEM fracture topography of a rejected sample at a higher magnification, showing transgranular cleavage fracture and manganese sulphide inclusions

- The qualitative microstructural examination indicated that all wheels samples were primarily composed of pearlite – 5% ferrite
- The non-metallic inclusion content of clean sample was slightly lower than that of rejected sample. However, more work still needs to be carried out using scanning electron microscopy (SEM) and transmission electron microscopy (TEM) to study in detail the morphology of the inclusions in the supplied wagon wheel samples
- The EDS spectrum of the clean sample identified the inclusions to be manganese sulphides (MnS) and oxides, whilst the rejected sample had a mixture of MnS, oxides, and alumina (Al₂O₃) inclusions. Excess quantities of aluminium produce alumina inclusions, which very hard and deleterious
- Impact properties in the axial direction are lower than in circumferential direction, and an improved impact toughness was shown by the clean sample
- All of the samples from sectioned test wheels had room-temperature Charpy impact toughness values below that of the Class B wheel steel. The fracture surface was characterized essentially by transgranular cleavage fracture.

Future work

Based on the results obtained in this investigation, the following work is recommended:

Qualitative and quantitative determination of inclusions in high-carbon steel alloy

- Sourcing of more samples/test wheels of different cleanliness from a local wagon wheel supplier
- A full metallurgical characterization (i.e. optical and fractography) and material property evaluation of the commercial alloy (Class B) from a local supplier
- Other mechanical tests such as fatigue and fracture toughness so that a cleanliness versus toughness curve can be produced
- SEM and TEM to study in detail the morphology of the inclusions in wagon wheels
- Development of a procedure to quantify the inclusion content as per the AAR M107/ASTM E1245 specification.

Acknowledgements

The authors would like to thank Mintek and the Ferrous and Base Metals Development Network of the Advanced Metals Initiative (AMI-FMDN) for their financial support and permission to publish this work. Mr Clive Jones and Mrs Daniela Bakalova from Scaw Metals SA are thanked for their generosity in supplying samples (commercial Class B alloy) and technical advice.

References

1. ASTM INTERNATIONAL. ASTM A504/A504M-07. Standard specification for wrought carbon steel wheels. West Conshohocken, USA, 2000.
2. ASTM INTERNATIONAL. ASTM E45-87. Standard practice for determining the inclusion content of steel. West Conshohocken, USA, 2000.
3. SINGH, U.P., POPLI, A.M., JAIN, D.K., ROY, B., and JHA, S. Influence of microalloying on mechanical and metallurgical properties of wear resistant coach and wagon wheel steel. *Journal of Materials Engineering and Performance*, vol. 12, 2003. pp. 573-580.
4. BILL, A., MITURA, K., KALOC, R., and ZARYBNICKY, O. Comparison of properties of the solid wheels and tyres in relation with their heat treatment and their chemical composition. *Proceedings of the 6th International Wheelset Congress*. Colorado Springs, CO, 22-26 Oct. 1978., vol. 1, pp. 2-2-1-2-2-16.
5. MARICH, S. Development of improved rail and wheel materials. *Seminar of Vanadium in Rail Steels*, Chicago, IL, Nov. 1979. p. 23.
6. DIRKS, B. and ENBLOM, R. Prediction of wheel profile wear and rolling contact fatigue for the Stockholm commuter train. *16th International Wheelset Congress*, Cape Town, March 14-19 2010
7. CLARKE, M. Wheel rolling contact fatigue and rim defects investigation to further knowledge of the causes of RCF and to determine control measures. *Rail Safety and Standards Board*, London, UK, 2008. pp. 6-13.
8. SCAW METALS SA. Private communication, 2011
9. MURAKAMI, Y. and ENDO, M. Effects of defects, inclusions and inhomogeneities on fatigue strength. *International Journal of Fatigue*, vol. 16, 1994. pp. 163-182.
10. ROBLES HERNÁNDEZ, F.C., CUMMINGS, S., KALAY, S., and STONE, D. Properties and microstructure of high performance wheels. *Wear*, vol. 271, 2011. pp. 374-381.
11. ASTM INTERNATIONAL. ASTM E23-72. Notched bar impact testing of metallic materials. West Conshohocken, USA, 2000.
12. PARIDA, N., DAS, S.K., and TARAFDER, S. Failure analysis of railroad wheels. *Engineering Failure Analysis*, vol. 16, 2009. pp. 1454-1460. ◆

Air Liquide - improving gold recovery through local expertise



Air Liquide Southern Africa
Tel: +2711 389 7000, Kobus Durand (Metallurgy Manager) +2711 389 7377
www.airliquide.co.za



Air Liquide is a leading innovator in the application of gases to assist the metallurgy industry.

The development of the **ALDOC** system for leaching gold leads to improved efficiencies, reduction in costs and a boost in profits.

ALDOC facilitates, monitors and controls the oxygen in cyanidation tanks with an efficient injection system that delivers flow-rate, purity, pressure, uptime and Dissolved Oxygen. Air Liquide has been developing the right technology for the mining and metallurgy industry for years and is a world leader in industrial gases.

AIR LIQUIDE'S summary of benefits

- Reduced Process Cost
- Quality
- Service
- Reduced Cyanide Consumptions
- Improved Kinetics
- Improved Recoveries

ALDOC

There is an Air Liquide solution that's right for you.